

MOL 36681

TITLE PAGE

**Characterization of an NBS1 C-terminal peptide that can inhibit ATM-mediated
DNA damage responses and enhance radiosensitivity**

Mickael J. Cariveau, Xi Tang, Xiao-Li Cui, and Bo Xu.

Department of Biochemistry and Molecular Biology, Southern Research Institute,
Birmingham, AL, 35205, Comprehensive Cancer Center, University of Alabama at
Birmingham, Birmingham, AL, 35205

Department of Genetics, LSU Health Sciences Center, New Orleans, 70112

MOL 36681

Running title: Targeting NBS1-ATM interaction for radiosensitization

Corresponding Author: Bo Xu MD, PhD
Southern Research Institute
Department of Biochemistry and Molecular Biology
2000 9th Avenue South
Birmingham, AL 35205
Phone: 205-581-2845
Fax: 205-581-2097
E-mail: xu@sri.org

Number of text pages: 26

Number of figures: 6

Number of references: 25

Abstract: 245

Introduction: 539

Discussion: 648

Abbreviations

ATM, ataxia telangiectasia mutated; NBS1, Nijmegen breakage syndrome; IR, ionizing radiation; PI-3K, phosphatidylinositol 3-Kinase; wtNIP, wild-type NBS1 inhibitory peptide; scNIP, scrambled NBS1 inhibitory peptide; DSBs, double strand breaks; A-T, Ataxia telangiectasia; FATC, FAT carboxy-terminal domain; MRN, Mre11, Rad50, NBS1 complex; DMEM, Dulbecco's Modified Eagle Media; FBS, fetal bovine serum; RPMI-1640, Roswell Park Memorial Institute-1640; CO₂, carbon dioxide; DMSO, dimethyl sulfoxide; TSD, target to source distance; Tris-HCL, tris-hydrochloric acid; NaCl, sodium chloride; EDTA, ethylenediaminetetraacetic acid, NP-40, Nonidet P-40; Na₃VO₄, sodium orthovanadate; NaF, sodium fluoride; PMSF, Phenylmethanesulfonyl fluoride; SDS, Sodium dodecyl sulfate; PBS, phosphate buffered saline; FITC, fluorescein isothiocyanate; ATR, ataxia telangiectasia related; ATRIP, ATR interacting protein; DNA-PK, DNA dependent protein kinase; siRNA, small interfering RNA.

MOL 36681

ABSTRACT

ATM and NBS1, mutation of which lead to the human autosomal recessive diseases, Ataxia Telangiectasia (A-T) and Nijmegen Breakage Syndrome (NBS), respectively, are essential elements in the cellular response to ionizing radiation (IR)-induced DNA damage. ATM is a member of the PI-3K kinase family and is activated by IR in an NBS1-dependent manner. The extreme C-terminus of NBS1 contains an evolutionarily conserved sequence motif that is critical for binding to and activation of ATM after IR. ATM phosphorylates a series of targets to initiate cell cycle arrest and promote cell survival in response to DNA damage. Therefore, targeting the NBS1-ATM interaction may lead to a novel approach for specific ATM inhibition and radiosensitization. We developed small peptides containing the conserved C-terminal sequence of NBS1 to investigate whether these peptides can interfere with the DNA damage pathway. We found that wild-type NBS1 inhibitory peptides (wtNIP) can abrogate NBS1-ATM association in the presence or absence of IR. We also found that cells exposed to wtNIP displayed a significant reduction in radiation-induced γ -H2AX and NBS1 focus formation compared to cells treated with control peptides, demonstrating that wtNIP possesses a strong inhibitory effect on ATM. The inhibitory effect of wtNIP also leads to a significant decrease in clonogenic survival in response to IR. Furthermore, wtNIP does not radiosensitize cells with defective ATM, suggesting a specific inhibition of ATM. Collectively, these data provide a proof of principle for the use of NBS1 C-terminal small peptides as specific ATM inhibitors and radiosensitizers.

MOL 36681

INTRODUCTION

The DNA damage response is controlled by a concise series of signaling events that result in activation of cell cycle checkpoints, DNA repair, and apoptosis. This network is composed of a number of gene products, which include sensors, transducers and effectors. DNA double strand breaks (DSBs) are detected by sensor molecules that trigger the activation of transducing kinases. Transducers then amplify the signals by phosphorylation of effector molecules to regulate the signaling cascades that initiate cell cycle checkpoints, influence DNA repair machinery, or trigger apoptotic pathways. One central element in the network is the *ATM* gene, mutation of which contributes to the human autosomal recessive disorder Ataxia-Telangiectasia (A-T) (Shiloh, 2003). A-T is characterized by progressive neuro-degeneration, a variable immunodeficiency, an extremely high predisposition to the development of lymphoid malignancies, and a hypersensitivity to IR. Cells derived from A-T patients show a variety of abnormalities, including cell cycle checkpoint defects, chromosomal instability and hypersensitivity in response to IR. *ATM* is remarkable for its large size and the existence of a sequence in its carboxyl terminus similar to PI-3 kinases. A family of genes, including *Tel1*, *Mec1* and *Rad3* in yeast, *Mei-41* in *Drosophila* and *ATR* and *DNA-PK* in vertebrates, are similar in size and carboxyl terminal kinase sequence, and are all involved in controlling DNA damage response (Abraham, 2001). The functional domains of the ATM protein includes several HEAT repeats that act as scaffolding for assembly of molecular components, a PI-3 like kinase domain that can phosphorylate serine/ threonine followed by glutamine (the S/T-Q consensus sequence), and a FAT carboxy-terminal domain (FATC) which may regulate protein activity and stability (Perry and Kleckner,

MOL 36681

2003). ATM activation requires functional NBS1 (Cerosaletti and Concannon, 2004; Cerosaletti *et al.*, 2006; Falck *et al.*, 2005; Difilippantonio *et al.*, 2005). Mutations in the *NBS1* gene are responsible for Nijmegen Breakage Syndrome (NBS), a hereditary disorder that imparts an increased predisposition to development of malignancy and a hypersensitivity to IR (Shiloh, 1997). NBS1 forms a complex with Mre11 and Rad50 to be called the MRN complex. MRN is highly conserved and it influences each aspect of chromosome break metabolism (Varon *et al.*, 1998). Studies have shown that the MRN complex can detect DNA double strand breaks and recruit ATM to damaged DNA molecules (Lee and Paull, 2004; Lee and Paull, 2005). The C-terminus motif of NBS1 contains a conserved sequence motif that binds to two of the HEAT repeats (HEAT repeats 2 and 7) of ATM. This interaction is essential to activate the kinase (Falck *et al.*, 2005).

Since the binding of NBS1 is critical for ATM to be functioning in response to DNA damage, we hypothesized that interfering with the NBS1-ATM interaction may block ATM activation and confer radiosensitization. To test this hypothesis, we developed several small peptides containing the conserved C-terminal sequence motif of NBS1, and fused them to a polyarginine internalization sequence. Herein we describe the characterization of the C-terminal NBS1 inhibitory peptide in terms of internalization, half-life, cellular cytotoxicity, effects on the DNA damage response and radiosensitivity. Collectively, these data may lead to a better understanding of the mechanisms that could be used to increase the radiosensitivity of cancer and provides data that could be rapidly translated into the development of novel radiosensitizing drugs.

MOL 36681

MATERIALS AND METHODS

Cell culture

Human tumor cell lines HeLa and DU-145 (ATCC, Manassas, VA), and human SV-40 transformed fibroblast cell line GM9607 (Corriell Cell Repositories, Camden, NJ) were maintained in exponential growth in DMEM-10%FBS, in a 5% CO₂ humidified atmosphere. The glioma cell line M059J (Corriell Cell Repositories) were maintained in exponential growth in RPMI-15%FBS, in a 5% CO₂ humidified atmosphere.

Peptides synthesis

All peptides were synthesized by Abgent (San Diego, CA) and labeled with a biotin tag at their N-terminus for detection *in vitro*. Three peptides were produced, one containing the polyarginine (R₉) internalization sequence alone, and a wild-type NBS1 inhibitory peptide (wtNIP) corresponding to amino acids 735-744 of human NBS1, and a random sequence peptide in which a.a. 735-744 of human NBS1 were scrambled (scNIP). The peptides were dissolved in DMSO, stored at -20°C, and reconstituted in DMEM-10% FBS prior to use.

Irradiation

An X-RAD 320 Irradiation Cabinet (Precision X-ray, East Haven, CT) was employed at 320KV and 160mA, with a 0.8mm Sn + 0.25mm Cu + 1.5mm Al (HVL \cong 3.7 Cu) filter at a TSD of 20cm and a dose rate of 3.4Gy/min. All irradiations were conducted under normal atmospheric pressure and temperature.

Immunoprecipitation and Western blotting

MOL 36681

For co-immunoprecipitation of ATM, NBS1 and MRE11, cells were lysed 1 hour in ice-cold lysis buffer, which consisted of 10 mM Tris-HCl (pH 7.5), 100 mM NaCl, 5 mM EDTA, 0.5% NP-40, 5 mM Na₃VO₄, 1 mM NaF, and 1 mM PMSF. After centrifugation, supernatants were incubated with indicated antibodies. After extensive washing with the lysis buffer, immunoprecipitates were analyzed by immunoblot using specific antibodies. For western blotting analysis, samples (cell lysates or immunoprecipitates) were separated on 4-12% SDS-poly-acrylamide gels, transferred to nitrocellulose membranes, and probed with various antibodies.

Immunofluorescence microscopy

Exponentially growing cultures of cells were plated on sterile, 22cm² coverslips, and incubated for 24 hours at 37°C in 5% CO₂ humidified air before they are treated with the NIP peptides at room temperature. Coverslips were washed with PBS and fixed with 4% paraformaldehyde-0.25% Triton X-100 for 15 minutes at room temperature, blocked for 30 minutes at room temperature, and incubated with FITC-conjugated streptavidin or anti- γ H2AX and phospho-NBS1 antibodies (Rockland Immunochemicals, Gilbertsville, PA) for 1 hour at room temperature. Coverslips were then mounted with Vectashield Elite (Vector Labs, Burlingame, CA) and observed with a Leica fluorescence microscope. Images were captured at 40 \times magnification using a Q Imaging Retiga Exi digital camera and analyzed with Image Pro-Plus 5.1 software.

MTT assay

For cytotoxicity studies, exponentially growing cultures of HeLa or DU-145 cells were harvested, plated in 96-well plates (5000 cells/well) in complete media, and incubated overnight. On the following day cells were treated with the NIP peptides (0,

MOL 36681

5, 10, 20, 50 or 100 μ M) or Taxol (0, 10, 50 or 100uM) as a positive control. At the end of the time course, an MTT cell viability assay (Promega Corp., Madison, WI) was used according to manufacturer's guidelines to determine peptide cytotoxicity.

Colony formation assays

To determine the radiosensitivity, the colony forming assay was incorporated. Cells were harvested with 0.125% trypsin-0.05% EDTA, pelleted and re-suspended in 1ml fresh media with a 22g needle to disperse clumps prior to hemocytometer counting in trypan blue. Cells were then plated at limiting dilutions in 6-well plates and allowed to adhere overnight. Cultures were treated with PBS, R₉, wtNIP, or scNIP for 1 hour, and irradiated (0-6Gy). Fresh peptides were added every four hours until 24 hours after IR, when the medium was replaced with peptide-free medium. Cultures were incubated for 10-12 days, harvested and stained with 0.5% crystal violet in methanol. Colony number was determined with a dissecting microscope. A population of >50 cells was counted as one colony, and the number of colonies was expressed as a percentage of the value for untreated mock irradiated control cells. The surviving curves were plotted by linear regression analyses and the D₀ value represents the radiation dose that leads to 37% of survival. To determine the radiosensitizing potential of the peptides in comparison to other small molecule inhibitors, we calculated the sensitizing enhancement ratio (SER) based on the dose of radiation required to reduce survival to 37% in the presence of scNIP or wtNIP. The following formula was used:

MOL 36681

$$\text{SER} = \frac{D_0 \text{ for scNIP treated cells}}{D_0 \text{ for wtNIP treated cells}}$$

Statistics

To establish statistical significance, Student's t-test was incorporated. The data were first fit to each experimental group over a dose range of 0-6Gy. Significant differences were established at $p < 0.05$.

MOL 36681

RESULTS

Internalization and cytotoxicity of the C-terminal NBS1 inhibitory peptides

Previous studies have revealed that the C-terminal NBS1 domain is critical for its binding to ATM and an NBS1 truncated derivative lacking the C-terminal 20 residues does not associate with ATM *in vitro* (Cerosaletti and Concannon, 2004;Cerosaletti *et al.*, 2006;Cerosaletti and Concannon, 2003;Falck *et al.*, 2005). In addition, it has been shown that expression of an NBS1 transgene lacking the ATM binding domain in NBS cells leads to a dramatic reduction in ATM activation (Difilippantonio *et al.*, 2005). Since inhibiting NBS1 association with ATM leads to suboptimal ATM activation after IR, the NBS1-ATM interaction can be a novel target for developing radiosensitizers. One approach to inhibiting NBS1-ATM interaction would be to use small peptides containing the conserved C-terminal sequence which will presumably compete with endogenous NBS1-ATM interactions (**Figure 1A**). Therefore we designed peptides containing two functional domains: one an interfering domain which will inhibit the NBS1-ATM association, and the other an internalization domain which will transport the interfering peptides into cells. For the interfering domain, we used the amino acid sequences containing the conserved C-terminal motif of NBS1 as shown in **Figure 1B**. This sequence contains the shortest ATM binding motif based on *in vitro* data (data not shown). For the internalization domain, we used a polyarginine sequence, which has been shown to have a significant efficiency of transporting small peptides and proteins across the plasma membrane (Deshayes *et al.*, 2005; Fuchs and Raines, 2004) Three peptides were generated, including the R₉-alone, and a wild-type NBS1 inhibitory peptide (wtNIP) corresponding to amino acids 735-744 of human NBS1. The third

MOL 36681

peptide was designed as a negative control, using a random sequence generator to produce a peptide in which a.a. 735-744 of NBS1 were scrambled (scNIP). These peptides were labeled with a biotin tag at their N-terminus for detection *in vitro*.

We first evaluated the internalization of the fusion peptides. Treatment of HeLa cells with R₉, wtNIP, or scNIP at a concentration of 10 μ M for 1hr led to a significant cellular uptake of peptide (**Figure 2**). R₉, wtNIP and scNIP internalization was localized to the cytoplasmic and nuclear compartments, while the control group, treated with DMEM alone shows no fluorescent signal. Since the peptides would be used in radiation studies, we then determined the length of time the peptides remain in cells to ensure the peptides would be present throughout the DNA repair process after IR. Cells treated with wtNIP or scNIP have significantly decreased fluorescence at 8 hours post-treatment (**Supplemental Figure 1**), suggesting that the NIP peptides should be added to cells every 4-6 hours in the first 24 hours after treatment with IR in order to achieve maximum inhibitory effects.

We then determined *in vitro* cytotoxicity of R₉, wtNIP and scNIP. HeLa cells grown in 96-well plates were treated with the peptides (0, 5, 10, 20, 50 or 100 μ M) or Taxol (0, 10, 20, 50 or 100 μ M) for 24hr. Following treatment, the MTT assay was used to measure the production of solubilized formazan, a metabolic indicator of cell proliferation. The peptides demonstrated no growth inhibitory or cytotoxic effects up to 72 hours after treatment (**Figure 2B**) when the peptide doses were lower than 20 μ M. Based on the cytotoxicity observed in the MTT assay, we chose 10 μ M as the working concentration for all subsequent experiments. The effect of 10 μ M R₉, wtNIP and scNIP on clonogenic survival displayed no significant difference between treatment groups

MOL 36681

($p < 0.05$) (Data not shown). It is noted that dose and time course experiments have been performed in several other cell lines and our data confirmed rapid internalization and minimal cytotoxicity of these peptides (data not shown).

wtNIP abrogates the NBS1-ATM interaction

To investigate whether R₉-conjugated NIP peptides can inhibit NBS1-ATM interactions, we performed co-immunoprecipitation experiments in cells treated with the NIP peptides. Four hours after peptide treatment, HeLa cells were harvested and subjected for immunoprecipitation using an anti-NBS1 antibody. The immunoprecipitates were then blotted with anti-ATM, NBS1 and MRE11 antibodies. We observed a normal level of ATM-NBS1 association in R₉ treated cells as compared to control cells. However, in wtNIP treated cells, NBS1 was no longer able to bring down ATM (**Figure 3**). Furthermore, the wtNIP only affect the NBS1-ATM interaction, and does not interfere with NBS1 binding to MRE11. In contrast, scNIP did not affect the NBS1-ATM interaction. In cells treated with IR, wtNIP showed a similar effect as in un-irradiated cells. These observations demonstrate that wtNIP can abrogate the NBS1-ATM interaction in the absence or the presence of DNA damage.

wtNIP inhibits IR-induced γ -H2AX and NBS1 pSer343 focus formation

One of the earliest responses to IR-induced DNA damage is the formation of γ -H2AX foci at sites of DSBs that requires functional ATM (Burma *et al.*, 2001; Furuta *et al.*, 2003). Since wtNIP showed an inhibitory effect on the NBS1-ATM interaction, we investigated whether IR-induced γ -H2AX focus formation was inhibited by the peptide.

MOL 36681

Immunofluorescence microscopy was used to detect the presence of γ -H2AX foci in mock or irradiated cells in the presence of R₉, wtNIP or scNIP. The average number of γ -H2AX foci/nucleus in HeLa cells significantly increased after IR in cells treated with R₉ (42 foci/nucleus) or scNIP (41 foci/nucleus), while cells treated with wtNIP displayed only an average of 6.9 γ -H2AX foci/nucleus, similar to that of mock-irradiated cells (**Figure 4**). Similar results were observed in DU-145 cells, whereas R₉ or scNIP exposure did not affect IR-induced focus formation and wtNIP showed significantly reduced H2AX foci/nucleus (**Supplemental Figure 2**). Therefore, IR-induced γ -H2AX focus formation can be inhibited by wtNIP.

To further support that wtNIP can inhibit ATM-mediated DNA damage pathways, we investigated IR-induced NBS1 focus formation, an event considered to be an ATM-dependent process at the sites of DSBs (Lim *et al.*, 2000). NBS1 foci are a result of ATM-mediated NBS1 phosphorylation on Serine 343. Using an anti-phospho-Ser343 NBS1 antibody, we observed that NBS1 phosphorylation was significantly inhibited in cells treated with wtNIP compared to those treated with R₉ or scNIP (**Figure 5A and supplemental Figure 3A**). The average number of foci in mock-irradiated HeLa cells was 6, 8, and 6 for R₉, wtNIP, and scNIP respectively. Cells treated with R₉ or scNIP displayed 25 and 31, while cells treated with wtNIP showed only 6 foci per nucleus after treatment with 6Gy IR (**Figure 5B**).

It is important to note that there was a low level of background focus formation for both NBS1 and γ -H2AX phosphorylation, which has been correlated to mitosis in normally growing mammalian cell cultures (McManus and Hendzel, 2005).

MOL 36681

wtNIP increases radiation sensitivity.

We then tested whether exposure to the NIP peptides will increase cellular radiosensitivity using the colony forming assay. **Figure 6A** depicts the survival curves for HeLa cells treated with R₉, wtNIP, or scNIP over a dose range of 0-6Gy. We found that neither R₉ nor scNIP affect radiosensitivity, while wtNIP can significantly decrease IR-induced survival. Radiation survival curves were characterized based on D₀ to define the NIP's effect on radiosensitivity. D₀ represents the mean lethal dose required for 37% survival, and is a measure of the intrinsic radiosensitivity of the cell. D₀ values for HeLa treated with wtNIP were 1.9 compared to 3.0 for cells treated with scNIP. To establish the statistical significance of wtNIP-induced radiosensitivity, Student's t-test (Paired 2 sample for means) was incorporated. The data were first fit to each experimental group over a dose range of 0-6Gy. Significant differences ($p < 0.05$) in clonogenic survival were observed between cells treated with wtNIP, and those treated with DMEM, R₉, or scNIP. The sensitization enhancement ratio (SER) was 1.58. This is comparable to other tested radiosensitizers, including gemcitabine, 5-fluorouracil, pentoxifylline, vinorelbine and some ATM-specific radiosensitizers with SERs from 1.1-2.5 (Lawrence *et al.*, 2001; Zhang *et al.*, 2004; Robinson and Shewach, 2001; Strunz *et al.*, 2002; Zhang *et al.*, 1998; Collis *et al.*, 2003). These observations have been confirmed in the prostate cancer cell line DU-145 (data not shown) with an SER of 1.46. Collectively, they provide strong evidence for the radiosensitizing potential of the wtNIP peptide.

Since wtNIP contains the conserved ATM binding sequence of NBS1, and this sequence is also conserved in the C-terminus of ATRIP and KU80, the interacting proteins of ATR and DNA-PKcs, respectively, it was possible that it might also inhibit

MOL 36681

ATR or DNA-PKcs (Abraham, 2001). To test this possibility, we performed colony forming assays in cell lines with defective ATM (GM9607) or DNA-PKcs (M059J). While treatment with wtNIP led to an increase in radiosensitivity in M059J cells (**Figure 6C**) with an SER of 1.83, GM9607 (**Figure 6D**) displayed no change in radiosensitivity. Since GM9607 cells are ATM-deficient and have functional ATR and DNA-PKcs, our observations strongly suggest that wtNIP can specifically target ATM, but not ATR or DNA-PKcs, to achieve radiosensitization.

MOL 36681

DISCUSSION

Because ATM is central to cellular responses to irradiation, blocking its activation or activity could make any type of tumor much more sensitive to radiation. Since cloning the gene in 1995, investigators have employed several methods to develop specific ATM inhibitors. These methods include antisense RNA, small interfering RNA (siRNA), and screening of small molecule inhibitors of ATM. Subcloning a full length cDNA of ATM in the opposite orientation into CB3AR cells significantly increased radiosensitivity (Zhang *et al.*, 1998). The development of siRNA also led to the generation of an siRNA that could inhibit ATM function in prostate cancer cells. Both DU-145 and PC-3 cells, when transfected with these plasmids, exhibited an increase in radiosensitivity at clinically relevant radiation doses (Collis *et al.*, 2003). More recently, the use of high throughput screening has provided a new generation of ATM inhibitors that can be quickly translated to clinical studies. By screening a combinatorial library of compounds around the DNA-PKcs inhibitor LY294002, Hickson *et al.* reported a compound (KU55933) to selectively inhibit the ATM kinase (Hickson *et al.*, 2004). Their studies have shown a significant increase in radiosensitivity in HeLa cells. However the *in vivo* radiosensitization effect and the toxicity of the compounds have not been reported.

Despite these promising findings, one of the major concerns of developing ATM inhibitors is the uncertainty of pleiotropic effects of such inhibitors. Due to the complex effects associated with malfunction of the protein kinase, the outcome of directly targeting ATM kinase activity can be complicated, as it is unclear whether the only effect of these reagents will be to confer radiosensitization.

MOL 36681

Instead of directly inhibiting the ATM kinase activity to increase radiosensitivity, an alternative approach is to target IR-induced ATM activation, as this will directly lead to an increase in radiosensitivity without interfering with other important functions of ATM in the absence of DNA damage. Since the NBS1-ATM interaction is important for IR-induced activation of ATM, selectively disrupting the signaling pathway would be a novel approach for developing radiosensitizers. Furthermore, since the C-terminal of NBS1 association with ATM is necessary for ATM activation, we reasoned that a small peptide containing a portion of this conserved C-terminal domain (i.e., **KEESLADDL**) would compete with the NBS1-ATM association *in vivo* and sensitize tumor cells to radiation. Our data demonstrate that the wild-type NBS1 peptide can be used to inhibit ATM activation and induce radiosensitization.

Since the wtNIP peptide contains the conserved sequence among the PI-3K kinase interacting proteins such as ATRIP and Ku80 (Falck *et al.*, 2005), we further reasoned a possibility that wtNIP could possibly interfere with ATR and DNA-PKcs activation. We tested the radiosensitizing effect of the peptides in cells with deficient ATM or DNA-PKcs. If the wtNIP could inhibit ATR or DNA-PKcs, then the ATM-deficient cells should be sensitized. However, the radiosensitivity of GM9607, which lacks of ATM but has functional ATR and DNA-PKcs, was not affected by the peptide. In contrast, the DNA-PKcs mutant cells showed an increased radiosensitivity similar to that of HeLa and DU-145 cells treated with wtNIP. These observations therefore demonstrate specific ATM inhibition by the wtNIP peptide.

In summary, we have established a proof of principle *in vitro*, with results that may lend insight into a novel approach to the development of powerful radiosensitizers

MOL 36681

for clinical cancer therapy and utilize the peptides as specific ATM inhibitors for further elucidation of signaling pathways involved in the DNA damage response. However, the use of the polyarginine-mediated NBS1 peptide as a therapeutic agent still faces challenges such as peptide stability, toxicity, tumor specific targeting, and immunogenic effects etc. Using the current concept to establish an assay for high throughput screening to identify small molecules that can target the NBS1-ATM interaction will eventually lead to novel radiosensitizers usable for clinical settings. Future studies are also necessary to determine the structure of the NBS1-ATM interaction complex and how wtNIP competes with the interaction.

MOL 36681

ACKNOWLEDGMENTS

We thank all members in the Xu lab for the technical help.

MOL 36681

References

- Abraham RT (2001) Cell Cycle Checkpoint Signaling Through the ATM and ATR Kinases. *Genes Dev* 15:2177-2196.
- Burma S, Chen B P, Murphy M, Kurimasa A and Chen D J (2001) ATM Phosphorylates Histone H2AX in Response to DNA Double-Strand Breaks. *J Biol Chem* 276:42462-42467.
- Cersaletti K and Concannon P (2004) Independent Roles for Nibrin and Mre11-Rad50 in the Activation and Function of Atm. *J Biol Chem* 279:38813-38819.
- Cersaletti K, Wright J and Concannon P (2006) Active Role for Nibrin in the Kinetics of Atm Activation. *Mol Cell Biol* 26:1691-1699.
- Cersaletti KM and Concannon P (2003) Nibrin Forkhead-Associated Domain and Breast Cancer C-Terminal Domain Are Both Required for Nuclear Focus Formation and Phosphorylation. *J Biol Chem* 278:21944-21951.
- Collis SJ, Swartz M J, Nelson W G and DeWeese T L (2003) Enhanced Radiation and Chemotherapy-Mediated Cell Killing of Human Cancer Cells by Small Inhibitory RNA Silencing of DNA Repair Factors. *Cancer Res* 63:1550-1554.
- Deshayes S, Morris M C, Divita G and Heitz F (2005) Cell-Penetrating Peptides: Tools for Intracellular Delivery of Therapeutics. *Cell Mol Life Sci* 62:1839-1849.
- Difilippantonio S, Celeste A, Fernandez-Capetillo O, Chen H T, Reina S M, Van Laethem F, Yang Y P, Petukhova G V, Eckhaus M, Feigenbaum L, Manova K, Kruhlak M, Camerini-Otero R D, Sharan S, Nussenzweig M and Nussenzweig A (2005) Role of Nbs1 in the Activation of the Atm Kinase Revealed in Humanized Mouse Models. *Nat Cell Biol* 7:675-685.
- Falck J, Coates J and Jackson S P (2005) Conserved Modes of Recruitment of ATM, ATR and DNA-PKcs to Sites of DNA Damage. *Nature* 434:605-611.
- Fuchs SM and Raines R T (2004) Pathway for Polyarginine Entry into Mammalian Cells. *Biochemistry* 43:2438-2444.
- Furuta T, Takemura H, Liao Z Y, Aune G J, Redon C, Sedelnikova O A, Pilch D R, Rogakou E P, Celeste A, Chen H T, Nussenzweig A, Aladjem M I, Bonner W M and Pommier Y (2003) Phosphorylation of Histone H2AX and Activation of Mre11, Rad50, and Nbs1 in Response to Replication-Dependent DNA Double-Strand Breaks Induced by Mammalian DNA Topoisomerase I Cleavage Complexes. *J Biol Chem* 278:20303-20312.
- Hickson I, Zhao Y, Richardson C J, Green S J, Martin N M, Orr A I, Reaper P M, Jackson S P, Curtin N J and Smith G C (2004) Identification and

MOL 36681

Characterization of a Novel and Specific Inhibitor of the Ataxia-Telangiectasia Mutated Kinase ATM. *Cancer Res* 64:9152-9159.

Lawrence TS, Davis M A, Hough A and Rehemtulla A (2001) The Role of Apoptosis in 2',2'-Difluoro-2'-Deoxycytidine (Gemcitabine)-Mediated Radiosensitization. *Clin Cancer Res* 7:314-319.

Lee JH and Paull T T (2004) Direct Activation of the ATM Protein Kinase by the Mre11/Rad50/Nbs1 Complex. *Science* 304:93-96.

Lee JH and Paull T T (2005) ATM Activation by DNA Double-Strand Breaks Through the Mre11-Rad50-Nbs1 Complex. *Science* 308:551-554.

McManus KJ and Hendzel M J (2005) ATM-Dependent DNA Damage-Independent Mitotic Phosphorylation of H2AX in Normally Growing Mammalian Cells. *Mol Biol Cell* 16:5013-5025.

Perry J and Kleckner N (2003) The ATRs, ATMs, and TORs Are Giant HEAT Repeat Proteins. *Cell* 112:151-155.

Robinson BW and Shewach D S (2001) Radiosensitization by Gemcitabine in P53 Wild-Type and Mutant MCF-7 Breast Carcinoma Cell Lines. *Clin Cancer Res* 7: 2581-2589.

Shiloh Y (1997) Ataxia-Telangiectasia and the Nijmegen Breakage Syndrome: Related Disorders but Genes Apart. *Annu Rev Genet* 31:635-662.

Shiloh Y (2003) ATM and Related Protein Kinases: Safeguarding Genome Integrity. *Nat Rev Cancer* 3: 155-168.

Stiff T, Reis C, Alderton G K, Woodbine L, O'Driscoll M and Jeggo P A (2005) Nbs1 Is Required for ATR-Dependent Phosphorylation Events. *EMBO J* 24:199-208.

Strunz AM, Peschke P, Waldeck W, Ehemann V, Kissel M and Debus J (2002) Preferential Radiosensitization in P53-Mutated Human Tumour Cell Lines by Pentoxifylline-Mediated Disruption of the G2/M Checkpoint Control. *Int J Radiat Biol* 78:721-732.

Varon R, Vissinga C, Platzer M, Cerosaletti K M, Chrzanoska K H, Saar K, Beckmann G, Seemanova E, Cooper P R, Nowak N J, Stumm M, Weemaes C M, Gatti R A, Wilson R K, Digweed M, Rosenthal A, Sperling K, Concannon P and Reis A (1998) Nibrin, a Novel DNA Double-Strand Break Repair Protein, Is Mutated in Nijmegen Breakage Syndrome. *Cell* 93:467-476.

Zhang M, Boyer M, Rivory L, Hong A, Clarke S, Stevens G and Fife K (2004) Radiosensitization of Vinorelbine and Gemcitabine in NCI-H460 Non-Small-Cell Lung Cancer Cells. *Int J Radiat Oncol Biol Phys* 58:353-360.

MOL 36681

Zhang N, Chen P, Gatei M, Scott S, Khanna K K and Lavin M F (1998) An Anti-Sense Construct of Full-Length ATM CDNA Imposes a Radiosensitive Phenotype on Normal Cells. *Oncogene* 17:811-818.

MOL 36681

FOOTNOTES

This work was supported in part by grants from the National Institutes of Health (RR020152-01 and ES013301), the Department of Defense W81XWH-05-1-0018 and the Strategic Investment Plan of Southern Research Institute.

Reprints should be sent to:
Bo Xu MD, PhD
Southern Research Institute
Department of Biochemistry and Molecular Biology
2000 9th Avenue South
Birmingham, AL 35205
Phone: 205-581-2845
Fax: 205-581-2097
E-mail: xu@sri.org

MOL 36681

LEGENDS FOR FIGURES

Figure 1. Development of the NBS1 inhibitory peptides

A. Schematic illustration of functional domains of ATM and NBS1 and their interaction. The C-terminal of NBS1 is required for ATM activation and recruitment to sites of DNA damage. It consists of at least two sets of amino acid residues, 736-737 (EE) and 741-742 (DDL), that are evolutionarily conserved and necessary for ATM binding. NBS1 binds to two sets of the Heat Repeats (Heat Repeat 2 (a.a. 248-522), and Heat Repeat 7 (a.a.1436-1770), in ATM. B. The amino acid sequences for the R₉, wtNIP, and scNIP peptides developed.

Figure 2. Peptide internalization and cytotoxicity

A. HeLa cells were treated with 10 μ M R₉, wtNIP, or scNIP for one hour and analyzed by immunofluorescence microscopy after staining with Fluorescein-conjugated streptavidin. B. HeLa cells were treated with Taxol and the NIP peptides at indicated doses. 24 hours after treatment, cell survival was quantified by a standard MTT assay.

Figure 3. wtNIP inhibits NBS1-ATM binding

HeLa cells treated with the NIP peptides were irradiated (0 or 6Gy). Immunoprecipitation was performed with a rabbit NBS1 antibody, and Western blotting was performed with monoclonal antibodies against ATM, NBS1 or MRE11.

MOL 36681

Figure 4. WtNIP can inhibit γ -H2AX focus formation

A. HeLa cells were treated with 10 μ M R₉, wtNIP, or scNIP for one hour, irradiated with 0 or 6Gy, and harvested 30 minutes later before immunofluorescence microscopy was employed to detect radiation induced- γ -H2AX foci. B. The mean γ -H2AX nuclear foci per nucleus were determined for each image using Image Pro 5.1 software and is expressed in arbitrary units. Error bars represent +/-1 SD, graphed are the mean of three independent experiments.

Figure 5. Exposure to the wtNIP peptide abrogates IR-induced NBS1 phosphorylation

A. HeLa cells were treated with 10 μ M R₉, wtNIP, or scNIP for one hour, irradiated with 0 or 6Gy, and harvested 120 minutes later before immunofluorescence microscopy was employed to detect radiation induced-NBS1 focus formation using an anti-Ser343 NBS1 antibody. B. The mean number of NBS1 foci per nucleus was determined from a population of at least 25 cells in three independent experiments. Error bars represent +/-1 SD, graphed are the mean of three independent experiments.

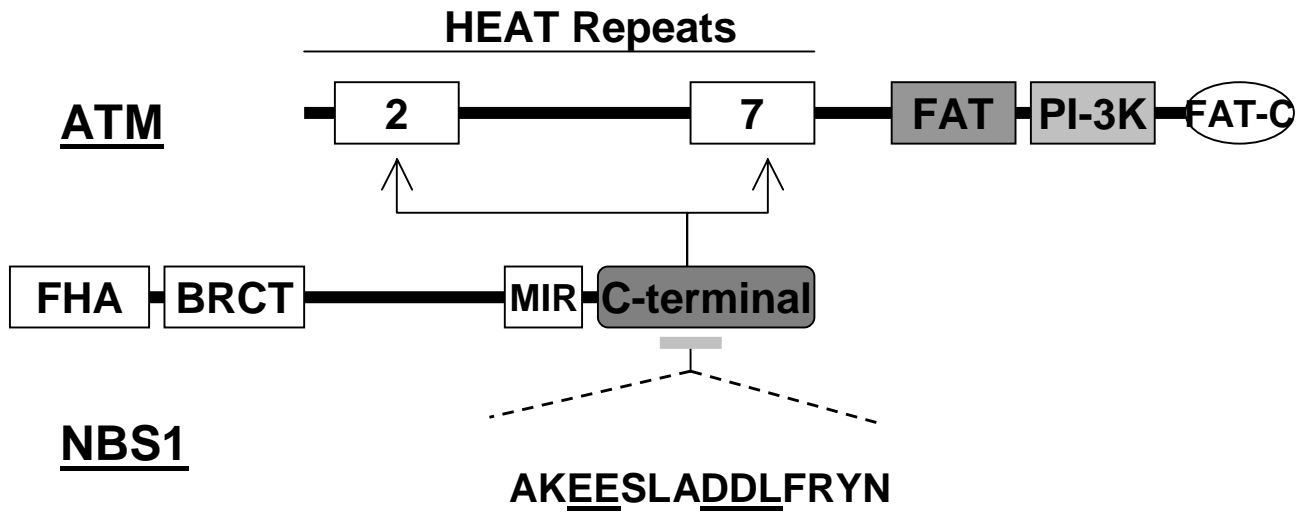
Figure 6. WtNIP increases cellular radiosensitivity

Cells were seeded at limiting dilutions and treated with 10 μ M R₉, wtNIP, or scNIP for one hour prior to irradiation, continuously exposed to the peptides for 24 hours, harvested 10-12 days later, and stained with crystal violet. Shown in **A** (HeLa), **C**

MOL 36681

(MO59J) and **D** (GM9607) are the surviving curves after indicated doses of radiation. Error bars represent +/- 1 SEM, graphed are the mean of three independent experiments. **B.** Representative plates of the clonogenic assay for NIP mediated radiosensitivity in HeLa cells.

A



B

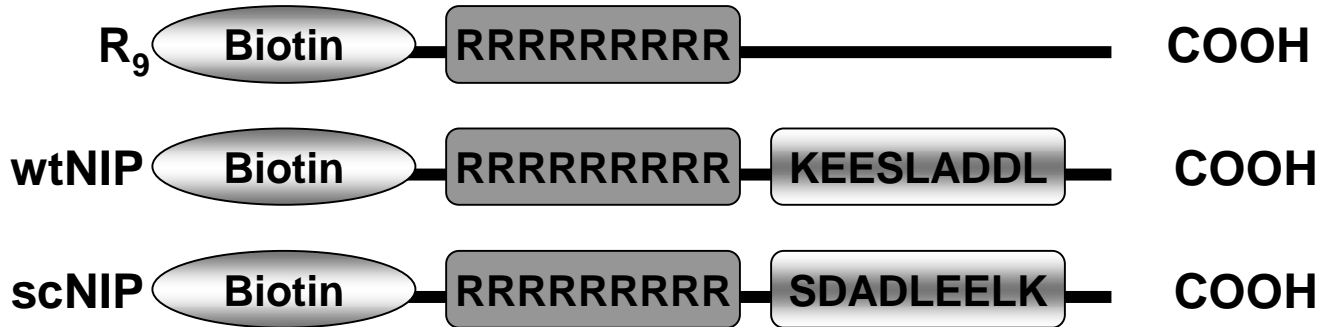


Figure 1

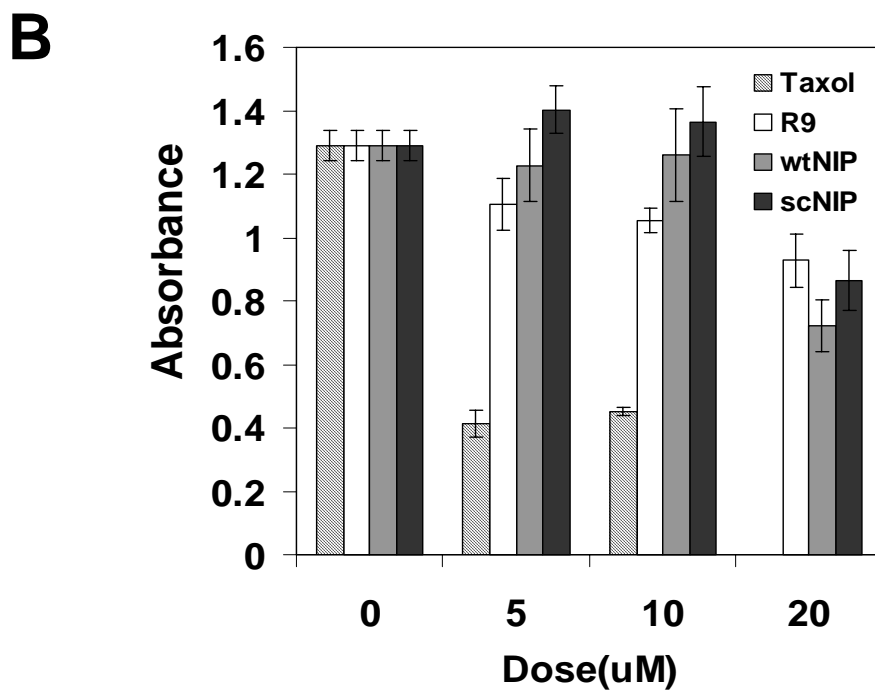
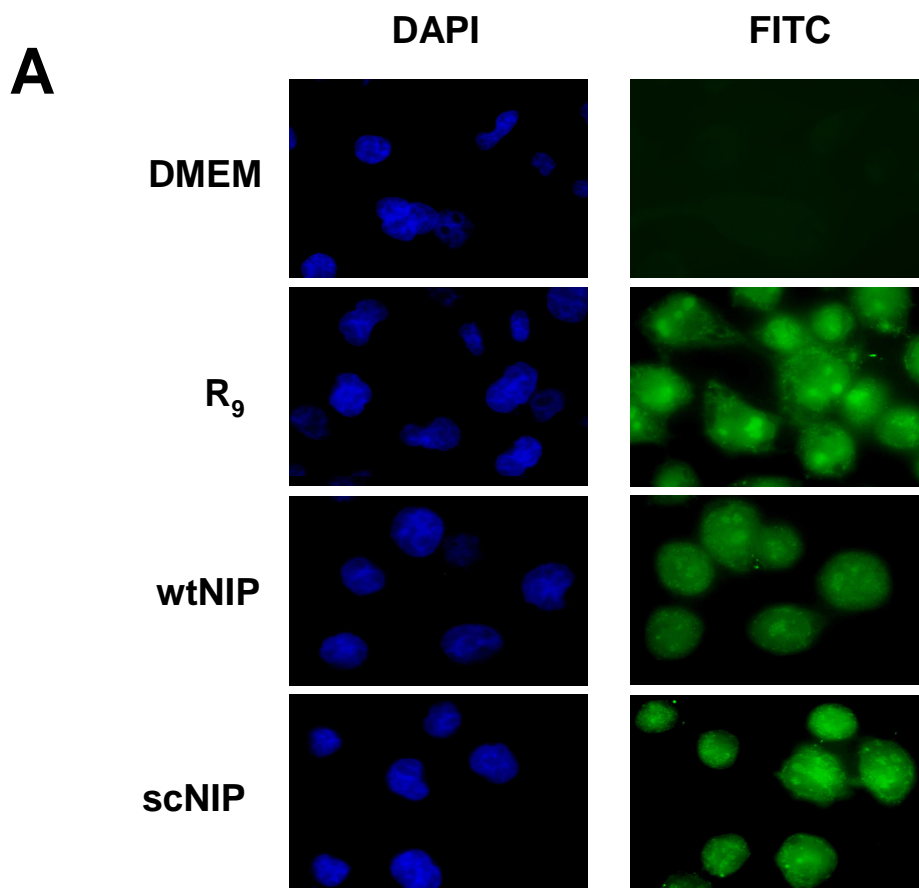


Figure 2

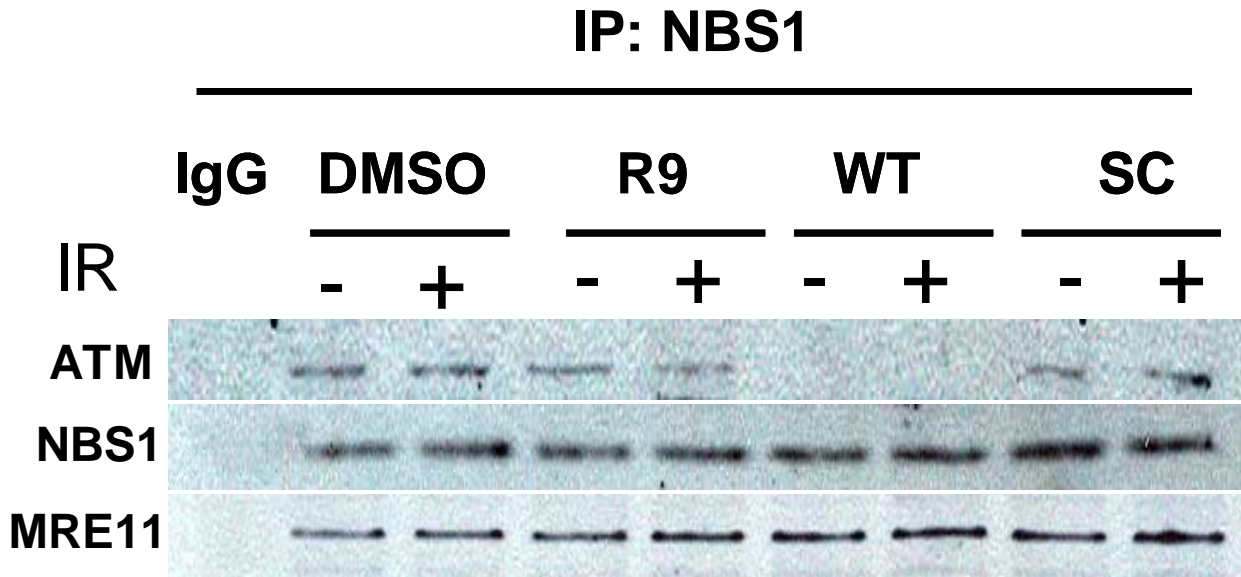
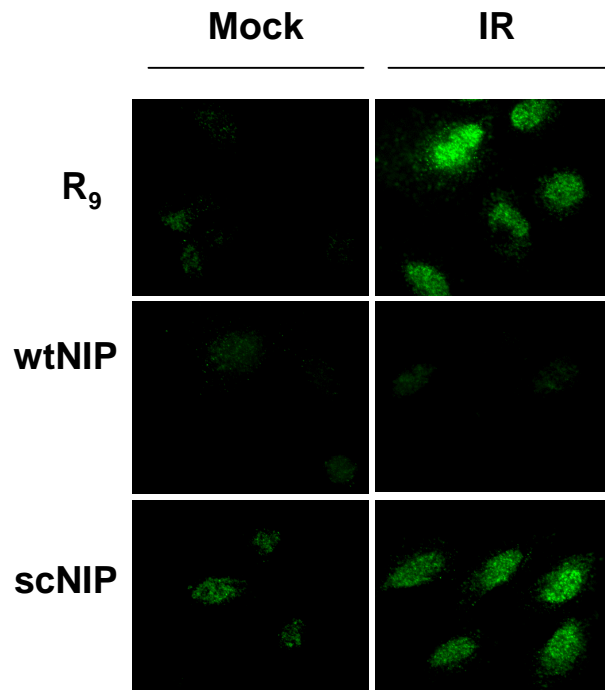


Figure 3

A



B

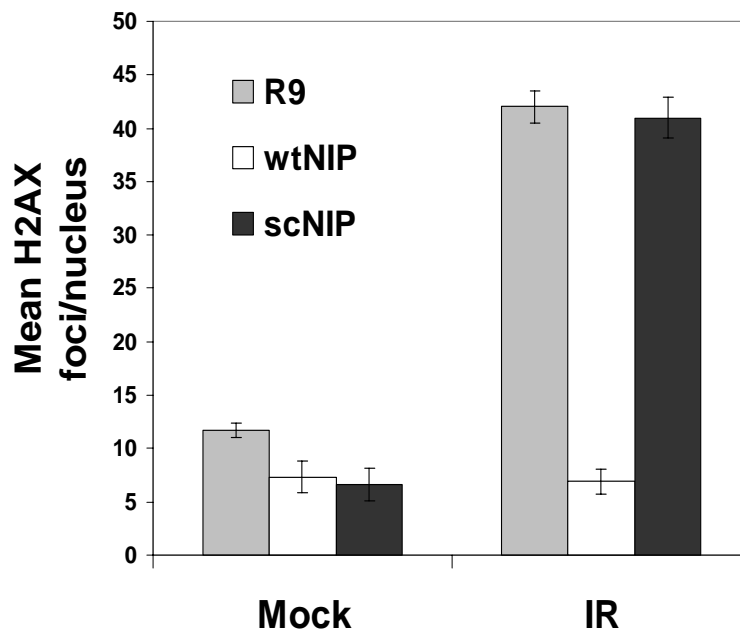


Figure 4

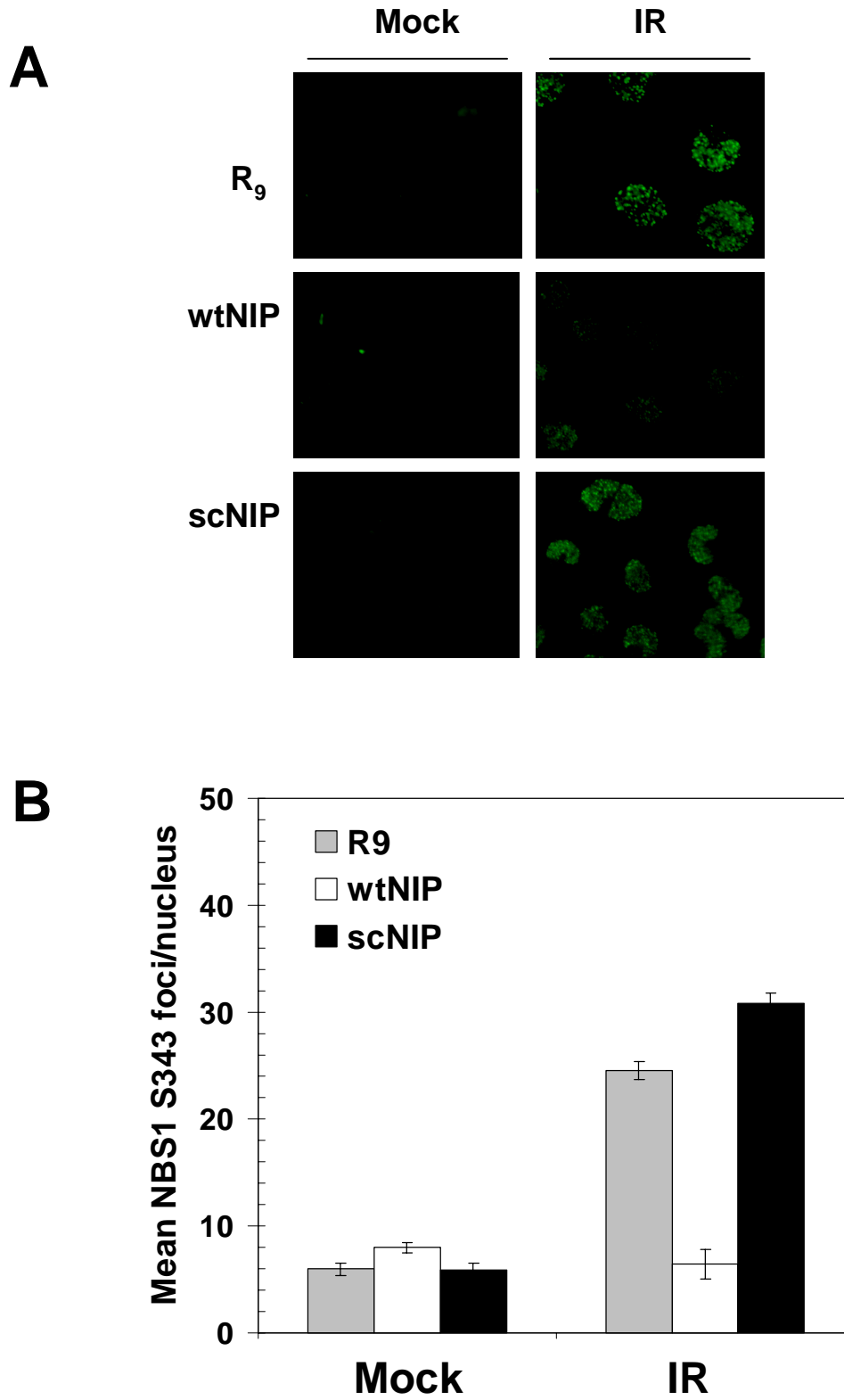


Figure 5

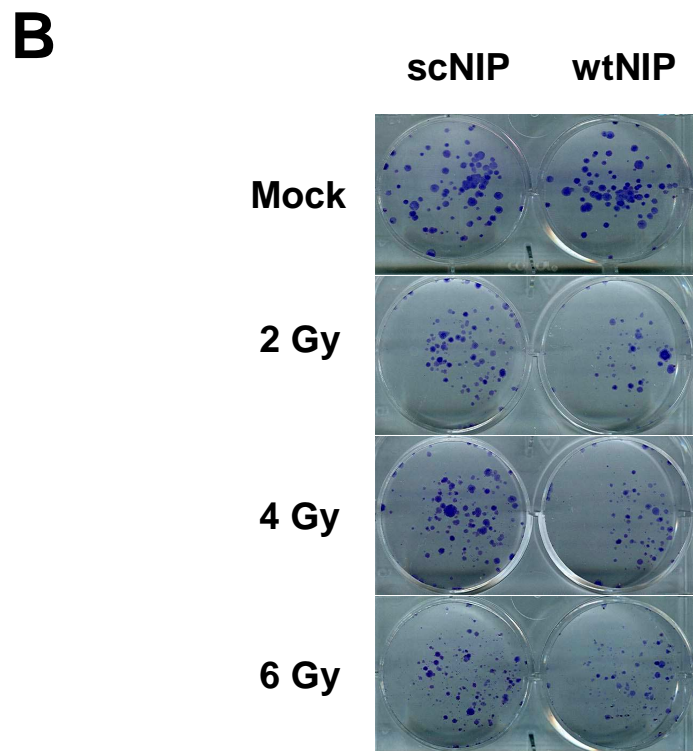
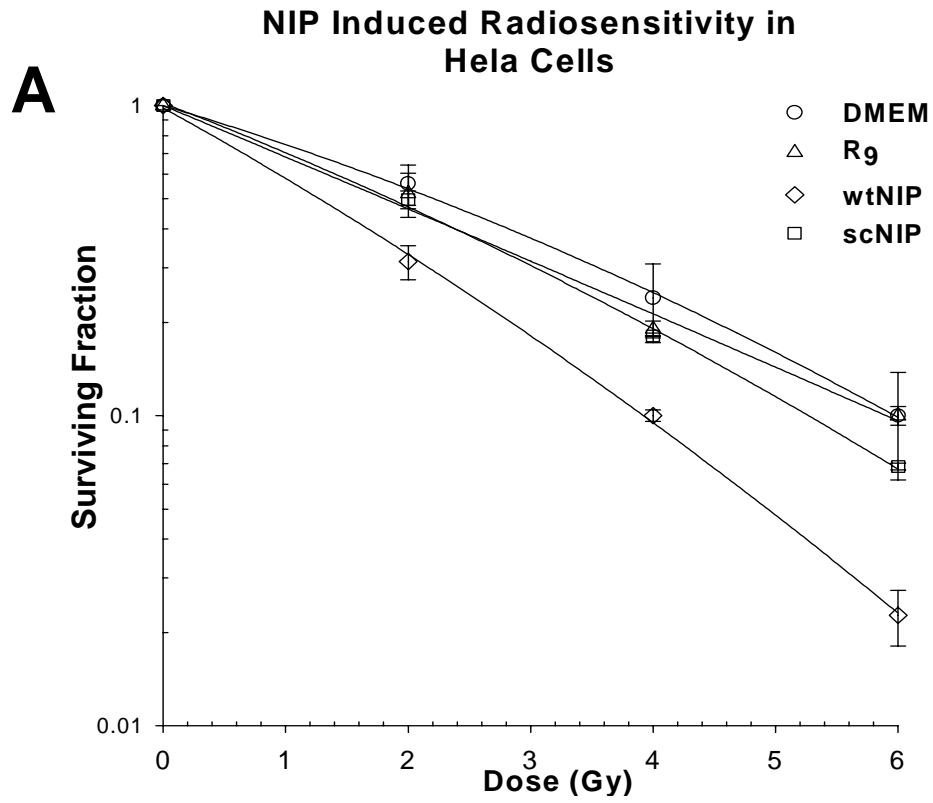


Figure 6

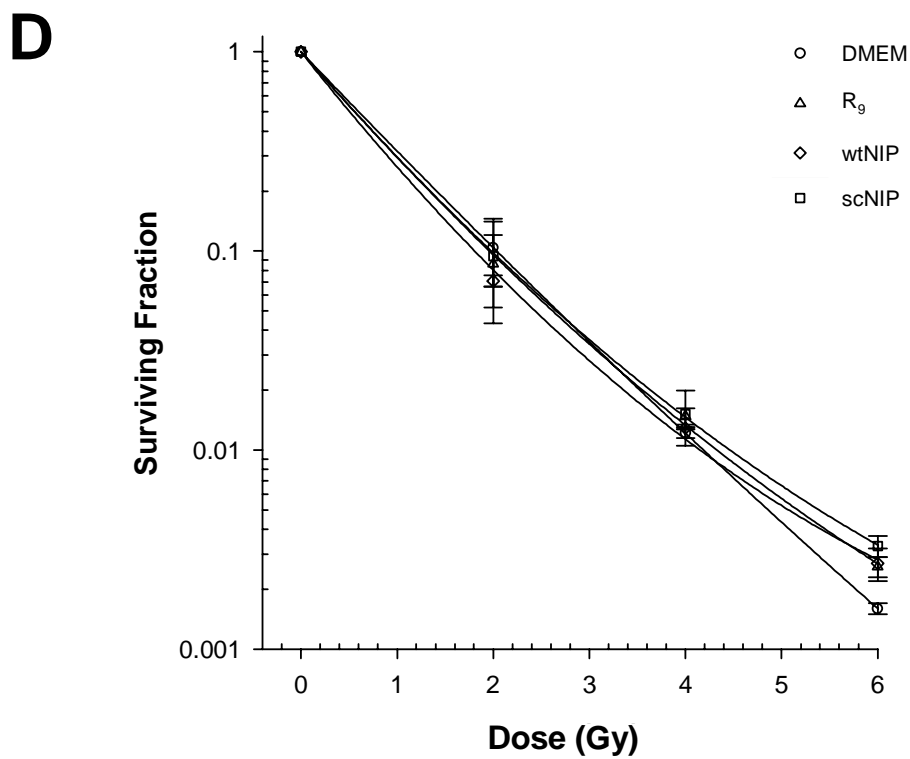
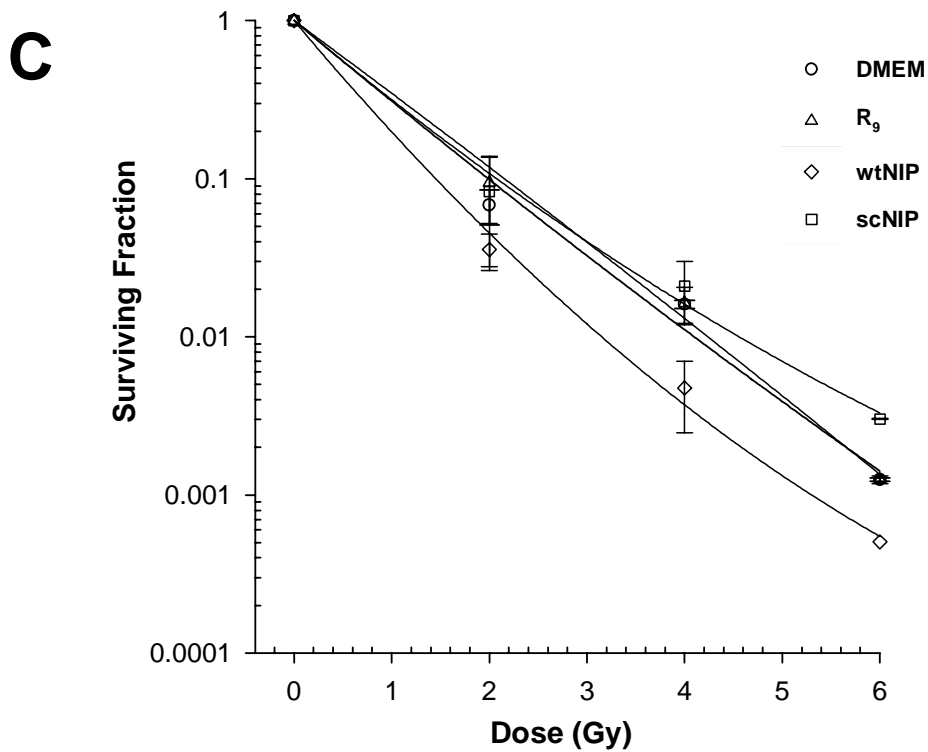


Figure 6